Quasioptical Fresnel-based lens antenna with frequency-steerable focal length for millimeter wave radars

Niklas Muckermann[1] , Jan Barowski[1] and Nils Pohl[1,2]

[1]Institute of Integrated Systems, Ruhr University Bochum, Bochum, Germany and [2]Fraunhofer FHR, Wachtberg, Germany

CAMBRIDGE UNIVERSITY PRESS

Abstract

This article presents the design of a dielectric lens antenna that utilizes the concept of a stepped Fresnel lens for focusing electromagnetic millimeter waves. Based on the quasi-optical properties of these waves, a Cartesian Oval is optimized and employed as a focusing lens. Multiple such lenses are combined to two different Fresnel-based lens antennas. We survey these newly designed lens antennas and compare them with a focusing lens antenna based on a Cartesian oval and a far-field lens antenna. Simulations and measurements with a frequency-modulated continuous-wave (FMCW) radar validate the effectiveness of the new design, demonstrating an even improved focus size while significantly reducing the size and weight of the lens antenna by up to 53% and by nearly 48 %, respectively. Additionally, the Fresnel-based lens antennas reveal a frequency dependency, enabling frequency-based steering of the focal length over a wide relative tuning range of 177%, which we thoroughly investigate for various bandwidths and center frequencies.

Introduction

A previous version of this paper was presented at the 52nd European Microwave Conference and published in its Proceedings [1]. Radar systems offer many possible applications and are often customized to meet specific requirements. One of the most important aspects is to guide the electromagnetic beam in a desired direction, as demonstrated in [2], and to shape it to achieve a focused beam or a collimated beam with a plane wavefront and high gain. This is, for example, utilized in reflector antennas with the transmitter or the receiver in the focal spot [3, 4]. Focusing is also applied in material characterization to selectively illuminate specific parts of a sample, as illustrated in [5] and [6]. Additionally, shaping electromagnetic beams finds applications in medical therapy for hyperthermia cancer treatment [7] and to enhance the range resolution of a radar system [8].

Redirecting or shaping of electromagnetic beams relies on passive components such as lenses and mirrors. Shaping through mirrors is either done by a curved mirror, as shown in [5] and [6] or by utilizing reflect arrays, which consist of arrays of microstrip patches [9], making reflect arrays thinner than curved mirrors.

Lenses, on the other hand, can be external systems, as used in [7, 8, 10–12] or lens antennas, as shown in [13–17]. Lens antennas are dielectric lenses designed to be directly mounted to devices like a radar system, offering the advantage of compactness and easy alignment compared to external components. In contrast, external lenses are positioned after an antenna, e.g., a horn antenna. This results in a more extended setup. To reduce the thickness of external lenses, similar to the use of reflect arrays instead of curved mirrors, Fresnel lenses are employed, as shown in [10, 11].

Requirements for focusing systems differ in their focal length and focal spot size. Some applications require relatively large focus distances compared to the employed electromagnetic wavelength and the desired focal spot size. These requirements arise from specific needs, such as maintaining a safety distance from moving parts in industrial environments [2], or because of distant targets within the human body, as discussed in [7]. Because of diffraction limits, this leads to large dimensions, no matter which focusing system is selected. Particularly lens antennas, where length and diameter depend on each other, become very large and therefore heavy. This increases material costs and makes manufacturing and subsequent handling more difficult. An alternative to conventional shaped lenses offer grooved and multi-dielectric Fresnel lenses as the authors of [10] and [11] use.

In this paper, we introduce a focusing lens antenna for millimeter waves that utilizes the idea of a stepped Fresnel lens, which is a new design approach to the best of the

authors' knowledge. The presented Fresnel-based lenses are smaller and therefore lighter than comparable focusing lens antennas and even achieve a smaller focal point radius. Furthermore, they have got a frequency dependence, allowing for steering the focal length.

Following in second section, we introduce essential quasioptical considerations for focusing lens antennas. Afterward in third section, we present the new Fresnel-based lens design and the manufactured lenses. In section "Simulation and Measurement Results," we show simulation and measurement results of these lenses and compare their different sizes and designs. After that, we investigate the frequency-dependence of the Fresnel-based lenses and examine how it can be utilized to steer the focal length.

Quasioptical considerations

To obtain a focusing lens antenna, the geometric shape of the lens must guide the electromagnetic waves in such a way that they converge. As in [15], we utilize a Cartesian oval to meet these requirements. A Cartesian oval possesses two focal points, one inside the oval and the other one outside. Figure 1 illustrates the cross-section of a focusing lens antenna that is based on a Cartesian oval. By rotating the 2-dimensional shape becomes a 3-dimensional object. The focal point inside the lens is used for feeding from a rectangular waveguide into the lens antenna. To achieve optimal matching, we utilize a stepped impedance transformer at the antenna feed, as the authors do in [13]. After propagating through the lens, the waves refract at the interface between the lens and air and converge to the focal point outside the lens, which is the desired geometric focus for the application.

The lens in Figure 1 is a Cartesian oval with the length l and the diameter D. The focal length f, which is the distance between the geometric focus and the largest diameter of the lens, is set by the shape of the Cartesian oval (see [15]). The resulting shape determines the front focal distance s_F, which is the distance between the beam waist and the vertex of the lens.

The former design considerations refer to the model of geometric optics, which describes the propagation of electromagnetic waves as rays but ignores the wave properties and effects by diffraction. This leads to deviations between the properties given by geometric optics and the actual behavior of the beam. A more precise description for focused electromagnetic millimeter waves is the paraxial solution of the wave equation as a Gaussian beam, which is valid for a beam radius $w_0 > 0.9 \cdot \lambda$ [18]. Figure 1 also
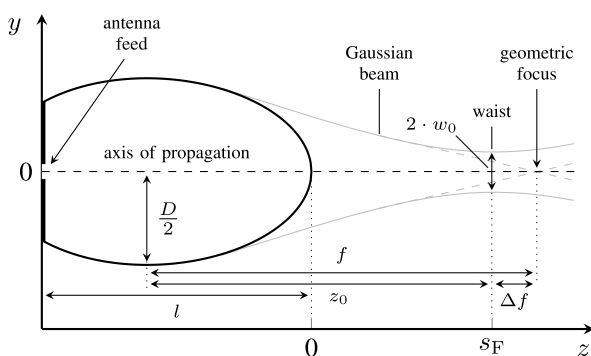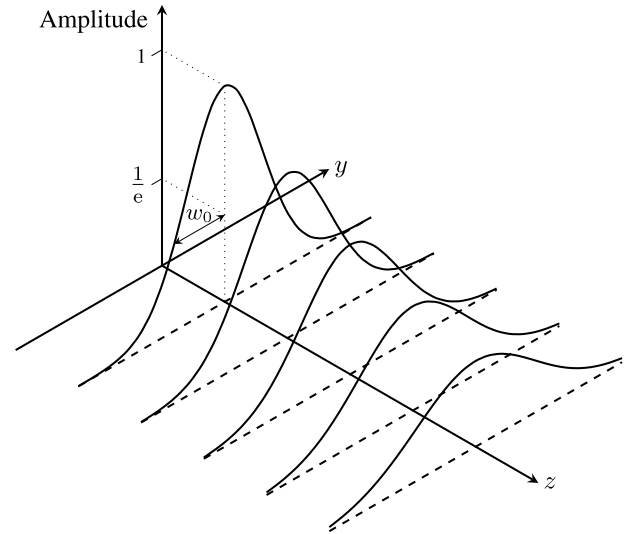
Figure 2. Amplitude profiles of Gaussian beam waists of focusing lenses with identical diameters D but increasing focal lengths in z-direction.

depicts the resulting Gaussian beam of a Cartesian oval, illustrating that the minimum radius

$$w_0 = \frac{2\lambda}{\pi} \cdot F_\#, \quad \text{with } F_\# = \frac{f}{D}, \tag{1}$$

occurs at the waist of the Gaussian beam and is not infinitely small. The beam waist w_0 is defined as the width from the axis of propagation to $\frac{1}{e^2}$ of the maximum intensity or $\frac{1}{e}$ of the maximum amplitude of the beam (see Figure 2). Equation (1) indicates that in order to achieve a narrow beam width, the F-number $F\#$ must be small. Conversely, a larger F-number results in a wider beam profile and a lower amplitude [18]. Figure 2 illustrates this aspect, displaying the Gaussian amplitude profiles at the beam waist for lenses with the same diameter D but increasing focal lengths in the z-direction, which leads to a bigger beam waist. To compensate for this effect, the diameter of the lens must increase, as equation (1) indicates.

Furthermore, the Gaussian beam differs from the geometric optics approach in that the waist of the former is positioned closer to the lens antenna than the geometric focus, as Figure 1 illustrates. According to [19], this difference can be quantified as follows:

$$\Delta f = f - z_0 = \frac{z_R^2}{z_0}. \tag{2}$$

In equation (2), z_0 represents the distance from the largest diameter of the lens to the beam waist (as Figure 1 shows), and z_R denotes the Rayleigh range. The Rayleigh range corresponds to the distance from the minimum area of the beam cross-section at the beam waist until it increases by a factor of two. It also characterizes the distance over which a Gaussian beam remains primarily collimated before it starts to diverge, and it indicates the point where the radius of curvature of the electromagnetic waves reaches its minimum. In [18] the author provides the following expression for the Rayleigh range:

$$z_R = \frac{\pi \cdot w_0^2}{\lambda}. \tag{3}$$

Inserting equation (3) with (1) into equation (2) gives

$$\Delta f = \frac{16 \cdot \lambda^2 \cdot f^4}{\pi^2 \cdot D^4 \cdot z_0}, \tag{4}$$

Figure 1. Cross-section of a focusing lens antenna, which is based on a Cartesian oval.

which implies that a small deviation Δf requires a short focal length or a large lens diameter, too.

Considering equations (1) and (4), it is evident that a large lens diameter D is necessary to achieve a narrow beam waist and minimize the deviation Δf, especially when the front focal distance, and thus the focal length, is large due to application-specific requirements. However, a large lens diameter also leads to an undesirably increased length l and, consequently, to a higher overall weight.
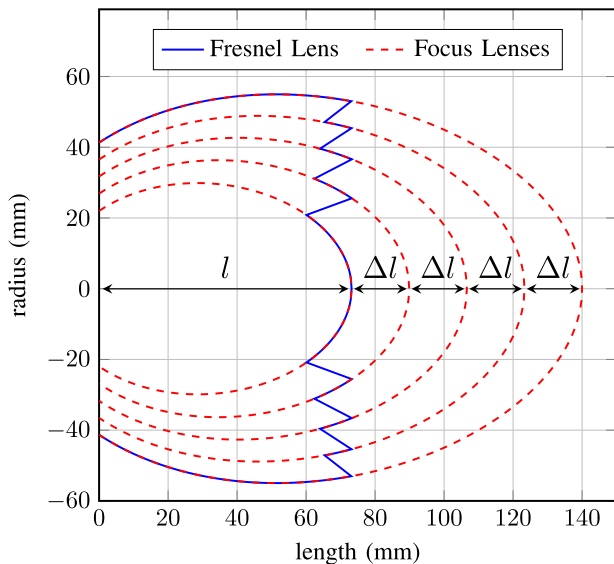

Figure 3. Design concept of the Fresnel-based lens antenna: Multiple focus lenses, with differing lengths l separated by Δl, are merged and subsequently trimmed to the length of the shortest lens.

Fresnel-based lens design

To overcome the disadvantage of large and heavy focus lens antennas, we propose a new lens design based on a stepped Fresnel lens as it is commonly used in optics to reduce the mass and volume of a conventional lens. The idea of a stepped Fresnel lens is to remove material that does not contribute to beam forming since only the surface of the lens refracts the beam. Therefore, the lens is divided into multiple circular areas and unnecessary material is removed, which forms the steps and makes the lens thinner.

Figure 3 presents our design concept for a Fresnel-based lens antenna. In contrast to a conventional Fresnel lens in optics, the introduced focus lens is based on a Cartesian oval and has two focal points. For all circular steps, all inner and all outer focal points must overlap constructively. Consequently, we designed each step as a circular area from a new lens with a different length l but the same distance between the antenna feed and the focal point outside the lens. Therefore, the length difference Δl between two consecutive lenses must be designed to achieve a constructive overlap, even though the electromagnetic waves have various propagation speeds and wavelengths through the air and the lens material. Since the Cartesian oval inherently ensures constructive interference for all beam paths between both focal points for one lens, it is sufficient to consider the most straightforward beam path between the inner and outer focal points to match multiple lenses to each other. This beam path is the direct one along the propagation axis, and it leads to a length difference between the individual lenses of

$$\Delta l = \lambda_{\text{air}}\left(n_1 + \frac{\Phi}{2\pi}\right) = \lambda_{\text{lens}}\left(n_2 + \frac{\Phi}{2\pi}\right), \qquad (5)$$

where λ_{air} and λ_{lens} are the wavelengths outside and inside the lens, n_1 and n_2 are the respective numbers of integer wavelengths within Δl. Φ is the phase shift, which has to be equal for the propagation inside and outside the lens.
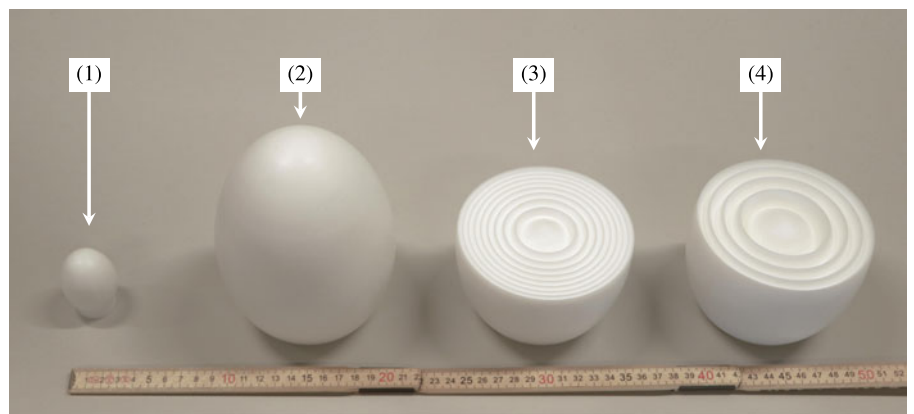
Figure 4. Investigated lenses: (1) far-field lens, (2) focus lens, (3) Fresnel lens with ten steps, (4) Fresnel lens with five steps.

Table 1. Properties of the investigated lenses from Figure 4

#	Lens	Length l (mm)	Diameter D (mm)	Weight (g)	z_0 (mm)	$w_{0,\text{calc}}$ (mm)	$w_{0,\text{meas}}$ (mm)	z_R (mm)
(1)	Far-field	42.3	36	73	–	–	–	–
(2)	Focus	140	112.9	2271	385.3	8.14	9	55.5
(3)	Focus-Fresnel	64.8	111.1	1188	310.5	6.67	6.8	37.3
(4)	Focus-Fresnel	73.2	111.3	1313	318.9	6.83	7.2	39.1

With Δl, we designed all lenses, starting from the original-sized focus lens, which is the largest and outermost, down to the smallest one. Whereas the smallest lens must be larger than the distance from the antenna feed to the largest diameter of the original-sized focus lens to retain the largest diameter D and the focusing properties. As equation (4) indicates, the difference Δf increases with decreasing lens diameters and increasing focal lengths, both of which applying to the shorter focus lenses. To compensate for this,
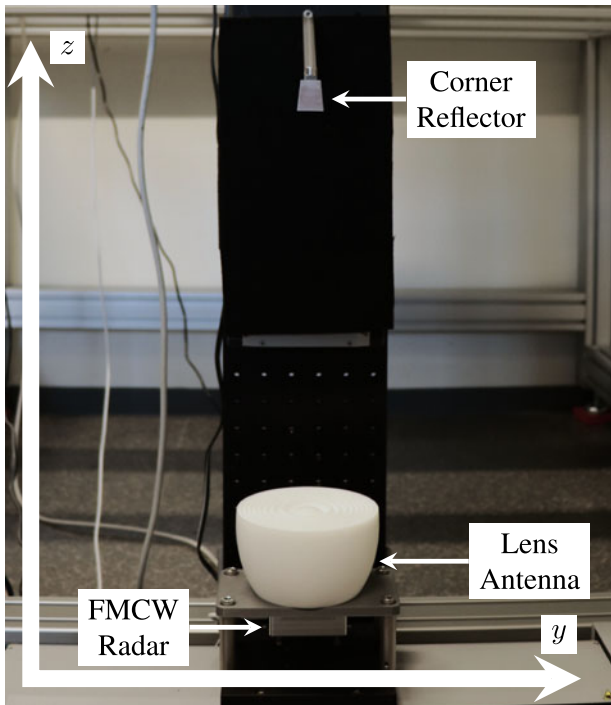

Figure 5. Measurement setup: FMCW radar with investigated lens antenna and a corner reflector with 20 mm side length on two perpendicular mounted linear track.

we utilized CST Microwave Studio to optimize the focus length of each focus lens, ensuring that their waists are positioned at the same location. Subsequently, we added all focus lenses together and cut the lenses to the size of the smallest lens. To prevent an inner smaller lens from shadowing an outer bigger lens, the transitions between the lenses are cut at an angle towards the feed of the antenna.

Figure 4 presents the in this work further investigated lenses. We designed all lenses for a center frequency of $f_c = 80$ GHz and used polytetrafluoroethylene (PTFE) as a dielectric material, because of its very low dissipation factor of $\tan(\delta) \approx 0.0002$, a relative permittivity of $\epsilon_r = 2.1$ and good machine processing properties. All lenses are manufactured through a turning process, and their properties are summarized in Table 1. Lens (1) is a small far-field lens, as the authors of [14] present. Lens (2) is a focus lens based on a Cartesian oval as Figure 1 depicts and presented in [15]. Lenses (3) and (4) are Fresnel lenses we made out of ten and five different-sized focus lenses, respectively, according to the design concept Figure 3 illustrates. Their outermost lenses have the same length as lens (2), before being cut to the size of the smallest lens. Lenses (2) to (4) have the same front focal distance of $s_F = 300$ mm, and therefore, lenses (3) and (4) have a shorter length z_0 than lens (2) and a slightly smaller diameter D (see Table 1). Together, this results in an up to 18 % smaller Gaussian beam radius $w_{0,\text{calc}}$, which we calculated with equation (1). Based on $w_{0,\text{calc}}$, we calculated the Rayleigh range z_R, which exhibits an even larger disparity between lens (2) and the Fresnel lenses. Lenses (2) to (4) differ not only in their focusing properties but also in their weight and length. Specifically, lenses (3) and (4) are 48% and 42% lighter and 54% and 48% shorter than lens (2).

Simulation and measurement results

We simulated and measured all lenses as shown in Figure 4. For the simulations we used CST Microwave Studio and for the measurements, we used a radar, which is an enhanced version of the in [20] and [21] proposed ultra-wideband FMCW radar with a center
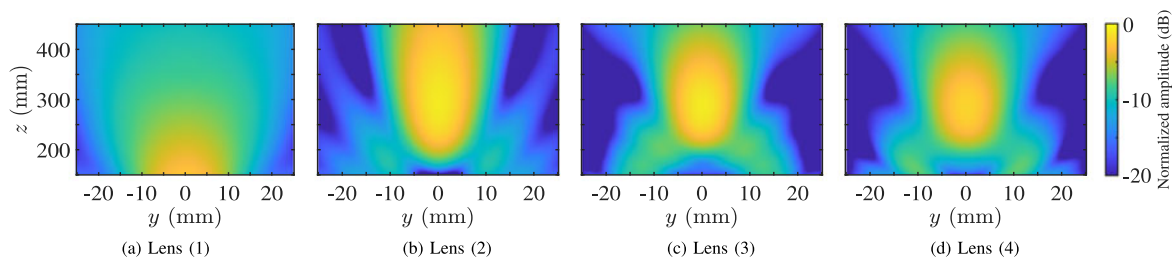

Figure 6. Simulated amplitudes of lens (1) to (4) in the yz-plane with a center frequency of $f_c = 80$ GHz, normalized to the maximum of lens (2) [1].
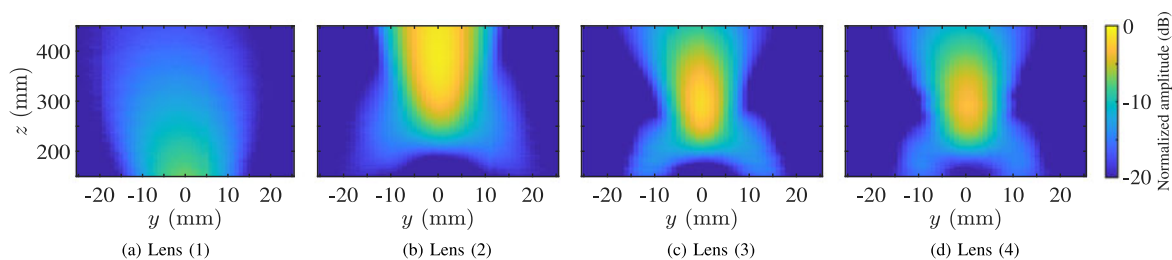

Figure 7. Measured amplitudes of lens (1)–(4) in the yz-plane with a center frequency of $f_c = 80$ GHz and a bandwidth of $B = 5$ GHz, normalized to the maximum of lens (2) [1].

frequency of 80 GHz, and a corner with a side length of 20 mm as a target. The radar and the corner are each mounted to a different linear track. The linear tracks are mounted so they move perpendicular to each other, as Figure 5 presents. In this manner,

the corner can be moved through the yz-plane of the investigated lenses.

Figures 6 and 7 present the simulated and measured normalized amplitudes in the yz-plane, with the reference point being at the apex of the respective lens in the rotational center, as illustrated in Figure 1. As one expects from the radar range equation, lens (1) has an amplitude drop with increasing distance. Conversely, lens (2) has a different behavior with a high amplitude at the focal length. The focal spot of lens (2) is limited in y- and z-direction, having a small width but an expanded length. In comparison, the focal spots of the Fresnel lenses are significantly shorter in the z-direction, as expected due to their shorter Rayleigh range, and have a smaller width (refer to Table 1). Comparing the measured results with the simulated ones demonstrates a strong agreement. The main lobes of the focusing lenses (2) to (4) are clearly visible, and the focal spots are comparable in size and amplitude. Only lens (2) exhibits a longer front focal distance in the measurement than expected based on the design and the simulated results. This discrepancy may be attributed to manufacturing deviations. The large size and the weight of lens (2) cause greater manufacturing challenges than the intricate contours of the Fresnel lenses (3) and (4), and even slight variations in the shape can affect the behavior of a lens of this size. Another difference between the simulated and measured results is the visibility of smaller amplitudes, which can be seen in the simulations but are not present in the measurements, resulting in missing side lobes, particularly noticeable in the focusing lenses. As the amplitude of the far-field lens (1) is lower than the one of the focusing lenses, the measurement results of lens (1) are also attenuated.

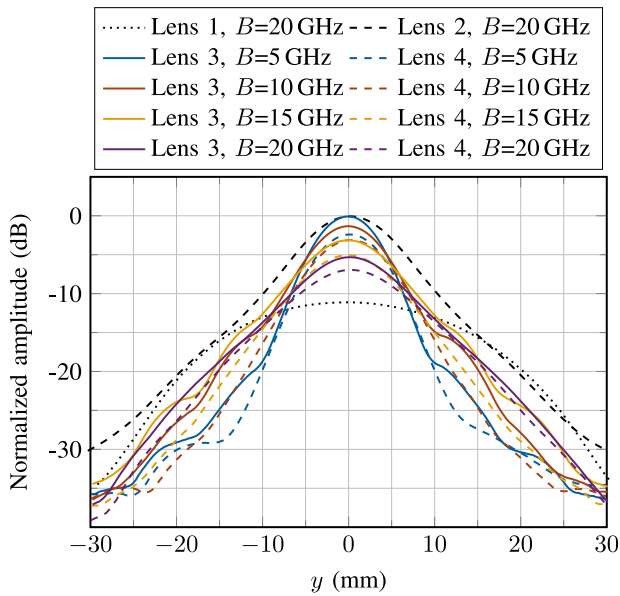**Figure 8.** Measured amplitudes of lens (1)–(4) over y with different bandwidths B, using a center frequency $f_c = 80$ GHz and a front focal distance $s_F = 300$ mm.

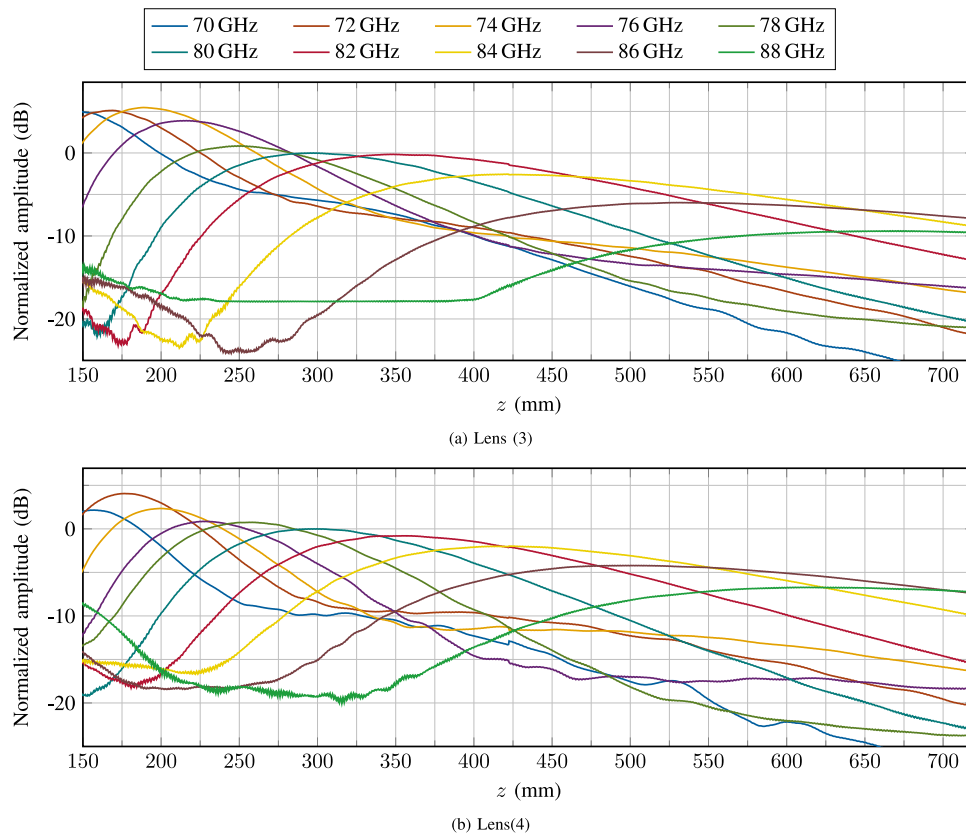(a) Lens (3)

(b) Lens(4)

Figure 9. Measured amplitudes of lenses (3) and (4) over z with different center frequencies f_c from 70 to 88 GHz and a constant bandwidth of $B = 4$ GHz, normalized to the maximum amplitude at $f_c = 80$ GHz.

Figure 10. Measured amplitudes of lenses (3) and (4) over y with different center frequencies f_c from 70 to 88 GHz and a constant bandwidth of $B = 4$ GHz, normalized to the maximum amplitude at $f_c = 80$ GHz.
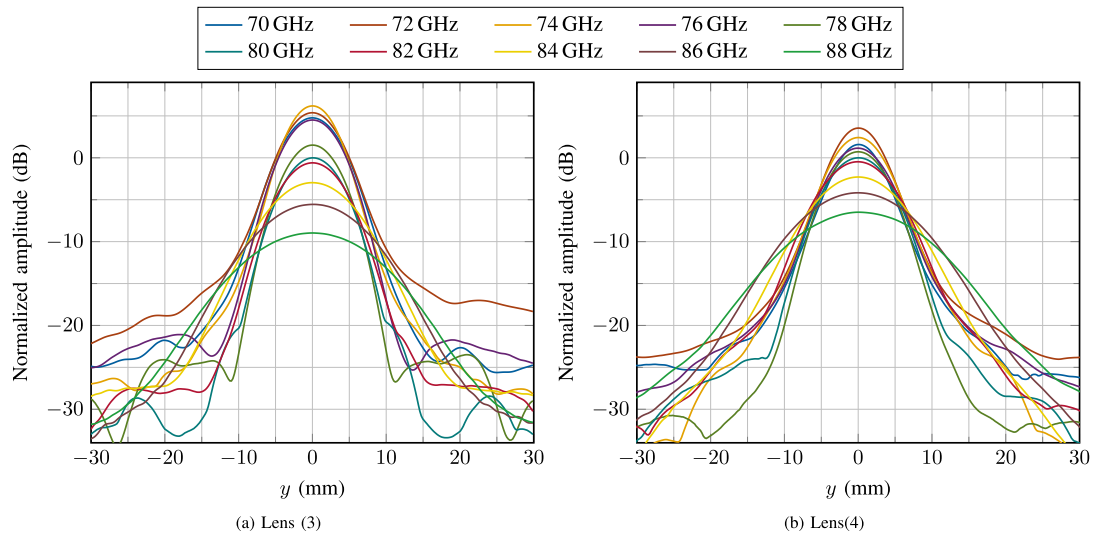
For further consideration, Figure 8 shows the amplitude over the y-axis at the front focal distance $s_F = 300$ mm for different bandwidths of the radar. Lens (2) at $B = 20$ GHz and lens (3) at $B = 5$ GHz have an equal maximum, but lens (3) has an over 24% smaller focus radius than lens (2), as it has been expected due to the shorter z_0 and the calculated beam radius $w_{0,calc}$. Lens (4) at $B = 5$ GHz also has a 20 % smaller focus radius than lens (2) but a smaller amplitude. The measured beam radius $w_{0,meas}$ of 9 mm, 6.8 mm and 7.2 mm for lens (2) at $B = 20$ GHz and lenses (3) and (4) at $B = 5$ GHz match well with the theoretical values in Table 1. Another visible aspect is the higher side lobe level (SLL) of lens (4) compared to lens (3). A noticeable effect for lens (4) appears at approximately ± 10 mm with an SLL of -26.6 dB, whereas the SLL for lens (3) is > -20 dB. The SLL of lens (1) and (2) cannot be determined, as their side lobes are not clearly identifiable.

As we presented in third section, the design rule in equation (5) is based on the wavelength to determine the length difference Δl between focus lenses the Fresnel lenses are made of. Consequently, the Fresnel lenses have a frequency dependence with varying properties for frequencies other than the design frequency of 80 GHz, as Figure 8 demonstrates. For higher bandwidths than $B = 5$ GHz and greater deviations from the center frequency, the focus radius increases while the amplitude decreases, implying a worse focus capability.

For further investigations on the frequency dependence of the Fresnel lenses, we examined lens (3) and lens (4) at various center frequencies f_c ranging from 70 GHz to 88 GHz with a small bandwidth of $B = 4$ GHz. Figures 9 and 10 show the amplitude along the z- and y-axis, respectively. All amplitudes are normalized to the maximum of the measurement with a center frequency $f_c = 80$ GHz.

In Figure 9 the measurements along the z-axis at $y = 0$ mm demonstrate the significant frequency dependence. For a center frequency of 80 GHz, which is the chosen frequency for the lens design, the peak is at the intended front focal distance of $s_F = 300$ mm. However, for increasing and decreasing center frequencies, the front focal distance also increases and decreases over a total range of 530 mm for lens (3) and 460 mm for lens (4). This represents a remarkably relative tuning range of 177% and 153%,
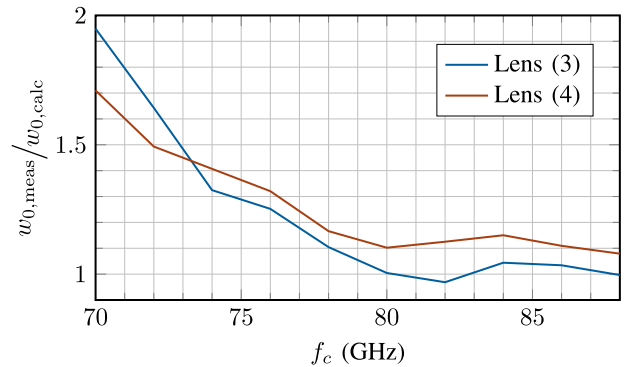
Figure 11. Measured waist radius $w_{0,meas}$ of lenses (3) and (4) over different center frequencies at a bandwidth of 4 GHz, referring the corresponding theoretical waist radius $w_{0,calc}$.
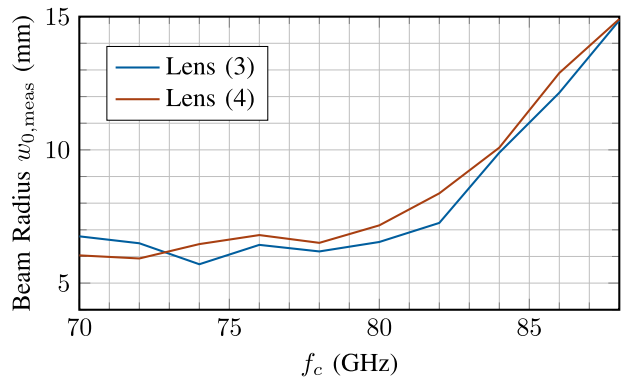
Figure 12. Measured beam waist radius $w_{0,meas}$ of lens (3) and lens (4) over different center frequencies at a bandwidth of 4 GHz.

respectively. In this regard, the amplitude decreases for larger front focal distances, and the focal spot becomes longer. The measurements in the y-direction at the corresponding focal points on the z-axis confirm this observation and demonstrate a widening of the beam waist for larger distances, as Figure 10 indicates. These results
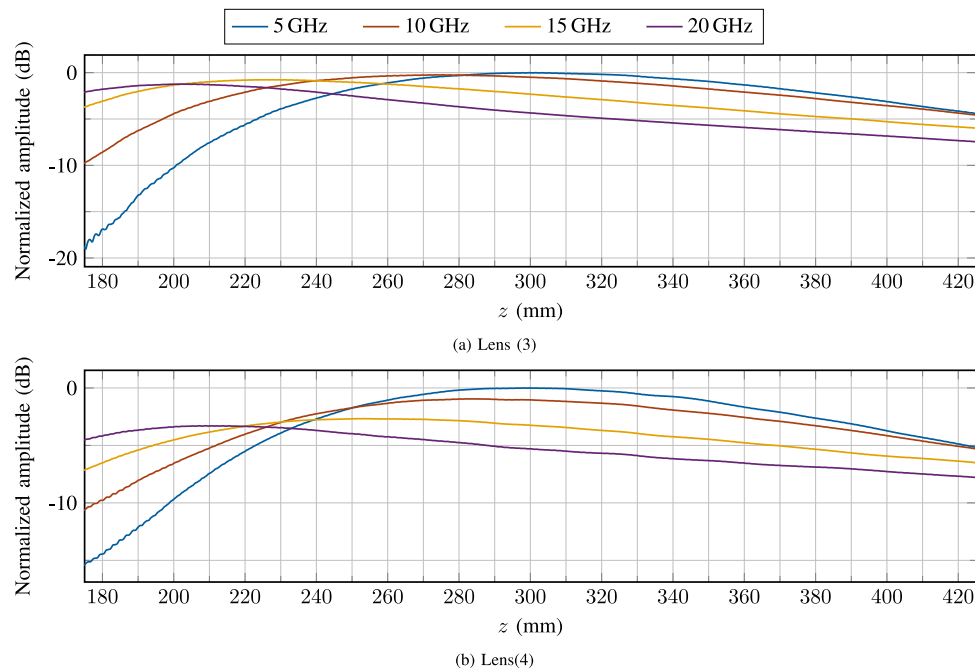
Figure 13. Measured amplitudes of lenses (3) and (4) over z with different bandwidths B and a center frequency of $f_c = 80\,\text{GHz}$, normalized to the maximum amplitude at $B = 5\,\text{GHz}$.

largely coincide with the theoretical considerations from Figure 2. Nevertheless, in both Figures 9 and 10, the highest amplitudes and narrowest beam waists are not achieved at the shortest focal length, but rather at a slightly higher center frequency.

Figure 11 depicts the ratio between the measured beam waist radius $w_{0,\text{meas}}$ and the theoretical value $w_{0,\text{calc}}$. Lens (3) and lens (4) exhibit only a minor deviation from the theoretical value for center frequencies $f_c > 80\,\text{GHz}$. For $f_c = 82\,\text{GHz}$, the measured beam radius of lens (3) is even smaller than the theoretical one, possibly attributable to the measurement setup's influence. In contrast, at center frequencies below 80 GHz, resulting in smaller front focal distances, the deviation increases noticeably. Nonetheless, despite the increasing deviation, the measured beam radius still exhibits a slight decrease, as Figure 12 demonstrates. It shows the measured beam radius as a function of the center frequency for both Fresnel lenses. Only for the lowest center frequencies the beam radius does increase again. Lens (3) has its minimum beam waist radius at a center frequency of 74 GHz and lens (4) at 72 GHz. These values correspond to the center frequencies with the highest amplitudes in Figures 9 and 10. For most center frequencies, lens (3) has a smaller beam radius compared to lens (4) and is closer to the theoretical value (see Figure 11). The smaller beam waist is due to shorter length z_0 of lens (3) compared to lens (4). However, for center frequencies under 73 GHz lens (4) achieves a smaller beam radius, although it has longer front focal distances for center frequencies $f_c < 80\,\text{GHz}$ than lens (3) as seen in Figure 9. One reason for this unexpected behavior might be the no longer correct shape of the individual Cartesian ovals of each Fresnel lens for front focal distances, which are a lot shorter than 300 mm.

The measurement results in Figures 9 and 10 illustrate the different focal lengths and beam radii for different center frequencies explaining the behavior in Figure 8 for higher bandwidths. As a higher bandwidth is a sweep through a larger spectrum of frequencies, more different focal lengths and beam radii occur in this measurement and add up to a wider beam with a lower amplitude. Figure 13 illustrates the result in z-direction for different

bandwidths at a center frequency of 80 GHz for the Fresnel lenses. The superposition can be seen here as well. For a small bandwidth of 5 GHz, the front focal distance remains at 300 mm. However, as the bandwidth increases, the focus size becomes longer while the amplitude and the front focal distance decrease, although Figure 2 indicates higher amplitudes and a smaller beam waists for shorter front focal distances. An explanation for the decreasing front focal distances with increasing bandwidths are the higher amplitudes for shorter front focal distances at smaller bandwidths as Figure 9 shows. Hence, the shorter front focal distances contribute more to the superimposed outcome.

Overall, these results highlight the excellent focusing properties of both Fresnel lenses and their ability to adjust their front focal distance over a vast range, although this frequency dependence admittedly leads to a decreased performance for higher bandwidths. Because of its smaller weight and size, narrower beam waist for most center frequencies, and a larger range for frequency steering, we suggest lens (3) for most applications.

Conclusion

We presented a novel concept for focusing lens antennas, based on a stepped Fresnel lens. Our approach uses the quasioptical characteristics of millimeter waves to design multiple focusing lenses based on geometric optics, which we optimized by simulation and joined together to a focusing Fresnel-based lens antenna. Our new design reduces the weight by up to 48% and the length by up to 54% compared to a Cartesian oval-based focusing lens with the same diameter and front focal distance. Subsequent measurements verify the focusing capabilities of the Fresnel lenses, even surpassing the comparable focus lens in terms of the minimum beam waist radius.

Furthermore, the special frequency-dependent design enables a steerable front focal distance by means of the center frequency over a considerable relative tuning range of up to 177%. The focus remains narrow for shorter front focal distances and stays close

to the theoretical limit for higher front focal distances. The frequency steering allows for a rapid and simple adjustment of the focal length without any hardware change, which can be useful for various applications in research, industry and medicine.

References

1. **Muckermann N, Barowski J and Pohl N** (2022) A large distance focus dielectric fresnel-based lens antenna for millimeter wave radar. In *2022 52nd European Microwave Conference (EuMC)*, Milan, Italy: IEEE, pp. 608–611.
2. **Muckermann N, Piotrowsky L and Pohl N** (2022) High accuracy thickness measurements of conducting material with single FMCW radar sensor. In *2022 14th German Microwave Conference (GeMiC)*, Ulm, Germany: IEEE, pp. 53–56.
3. **Takano T, Ogawa E, Betsudan S and Sato S** (1980) High efficiency and low sidelobe design for a large aperture offset reflector antenna. *IEEE Transactions on Antennas and Propagation* **28**(4), 460–466.
4. **Hannan P** (1961) Microwave antennas derived from the cassegrain telescope. *IRE Transactions on Antennas and Propagation* **9**(2), 140–153.
5. **Barowski J, Zimmermanns M and Rolfes I** (2018) Millimeter-wave characterization of dielectric materials using calibrated FMCW transceivers. *IEEE Transactions on Microwave Theory and Techniques* **66**(8), 3683–3689.
6. **Jebramcik J, J Barowski, J Wagner and I Rolfes** (2019) Radar based material characterization at 145 GHz utilizing an ellipsoidal reflector. In *2019 49th European Microwave Conference (EuMC)*. Paris, France: IEEE.
7. **Rahman AA, Kamardin K and Yamada Y** (2020) Focal spot size evaluation of a focused lens in human body. In *2020 IEEE International RF and Microwave Conference (RFM)*, Kuala Lumpur, Malaysia: IEEE, pp. 1–4.
8. **Altmann M and Ott P** (2017) Confocal radar system for improved FMCW range resolution. In *2017 International Conference on Research and Education in Mechatronics (REM)*, Wolfenbuettel, Germany: IEEE, pp. 1–4.
9. **Pozar D, Targonski S and Syrigos H** (1997) Design of millimeter wave microstrip reflectarrays. *IEEE Transactions on Antennas and Propagation* **45**(2), 287–296.
10. **Reid DR and Smith GS** (2007) A full electromagnetic analysis of grooved-dielectric fresnel zone plate antennas for microwave and millimeter-wave applications. *IEEE Transactions on Antennas and Propagation* **55**(8), 2138–2146.
11. **Jouade A, Himdi M and Lafond O** (2017) Fresnel lens at millimeter-wave: Enhancement of efficiency and radiation frequency bandwidth. *IEEE Transactions on Antennas and Propagation* **65**(11), 5776–5786.
12. **Mateo-Segura C, Dyke A, Dyke H, Haq S and Hao Y** (2014) Flat luneburg lens via transformation optics for directive antenna applications. *IEEE Transactions on Antennas and Propagation* **62**(4), 1945–1953.
13. **Pohl N** (2010) A dielectric lens antenna with enhanced aperture efficiency for industrial radar applications. In *IEEE Middle East Conference on Antennas and Propagation (MECAP 2010)*, Cairo, Egypt: IEEE, pp. 1–5.
14. **Pohl N and Gerding M** (2012) A dielectric lens-based antenna concept for high-precision industrial radar measurements at 24 GHz. In *2012 9th European Radar Conference*, Amsterdam, Netherlands: IEEE, pp. 405–408.
15. **Garten O, Barowski J and Rolfes I** (2020) Simulation and optimization of the design of focusing dielectric lenses based on cartesian ovals with physical optics. In *2020 International Workshop on Antenna Technology (iWAT)*, Bucharest, Romania: IEEE, pp. 1–4.
16. **Schulz C, Baer C, Pohl N, Musch T, Will B and Rolfes I** (2013) A multi directional dielectric lens approach for antennas used in industrial radar applications. In *2013 International Workshop on Antenna Technology (iWAT)*, Karlsruhe, Germany: IEEE, pp. 328–331.
17. **Mozharovskiy A, Artemenko A, Ssorin V, Maslennikov R and Sevastyanov A** (2015) High gain millimeter-wave lens antennas with improved aperture efficiency. In *2015 9th European Conference on Antennas and Propagation (EuCAP)*, Lisbon, Portugal: IEEE, pp. 1–5.
18. **Goldsmith P** (1992) Quasi-optical techniques. *Proceedings of the IEEE* **80**(11), 1729–1747.
19. **Siegman AE** (1986) *Lasers*. Sausalito, CA: University Science Books.
20. **Pohl N, Jaeschke T and Aufinger K** (2012) An ultra-wideband 80 GHz FMCW radar system using a SiGe bipolar transceiver chip stabilized by a fractional-n PLL synthesizer. *IEEE Transactions on Microwave Theory and Techniques* **60**(3), 757–765.
21. **Pohl N, Jaeschke T, Kuppers S, Bredendiek C and Nusler D** (2018) A compact ultra-wideband mmWave radar sensor at 80 GHz based on a SiGe transceiver chip (focused session on highly-integrated millimeter-wave radar sensors in SiGe BiCMOS technologies). In *2018 22nd International Microwave and Radar Conference (MIKON)*. Poznan, Poland: IEEE.

Niklas Muckermann received the B.Eng. degree from Ostfalia University of Applied Sciences, Wolfenbüttel, Germany, in 2018, and the M.Sc. degree in electrical and information engineering from Ruhr University Bochum, Bochum, Germany in 2021. Since 2021, he has been a Research Assistant with the Institute of Integrated Systems, Ruhr University Bochum. His current research interests include radar system design, embedded signal processing and concepts for radar systems in industrial applications.

Jan Barowski was born in Bochum, Germany, in 1988. He received the B.Sc. and M.Sc. degrees in electrical engineering and the Dr.Ing. degree (with honors) in electrical engineering from Ruhr University Bochum, Bochum, Germany, in 2010, 2012, and 2017, respectively. Since 2012, he has been with the Institute of Microwave Systems, headed by Ilona Rolfes, Ruhr University Bochum, as a Research Assistant. He is currently a Postdoctoral Research Scientist with the Institute of Microwave Systems. His research interests include radar signal processing, radar imaging, and material characterization techniques. Dr. Barowski was the recipient of the IEEE Antennas and Propagation Society Doctoral Research Grant in 2016 and the IEEE MTT IWMS-AMP Best Student Paper Award in 2017, U.R.S.I. Germany Sections Young Scientist Award and the German Association for Electrical, Electronic and Information Technologies (VDE) Award for the Doctoral dissertation, in 2018.

Nils Pohl received the Dipl.-Ing. and Dr.Ing. degrees in electrical engineering from Ruhr University Bochum, Bochum, Germany, in 2005 and 2010, respectively. From 2006 to 2011, he was a Research Assistant with Ruhr University Bochum, where he was involved in integrated circuits for millimeter-wave (mm-wave) radar applications. In 2011, he became an Assistant Professor with Ruhr University Bochum. In 2013, he became the Head of the Department of mm-wave Radar and High Frequency Sensors with the Fraunhofer FHR, Wachtberg, Germany. In 2016, he became a Full Professor for Integrated Systems with Ruhr University Bochum. In parallel, he is head of the Research group for Integrated Radar Sensors at Fraunhofer FHR. He has authored or coauthored more than 200 scientific papers and has issued several patents. His current research interests include ultra-wideband mm-wave radar, design, and optimization of mm-wave integrated SiGe circuits and system concepts with frequencies up to 500 GHz and above, as well as frequency synthesis and antennas. Prof. Pohl is a member of IEEE, VDE, ITG, EUMA, and URSI. He was a co-recipient of the 2009 EEEfCom Innovation Award, and a recipient of the Karl-Arnold Award of the North Rhine-Westphalian Academy of Sciences, Humanities and the Arts in 2013 and the IEEE MTT Outstanding Young Engineer Award in 2018. Additionally, he was co-recipient of the best paper award at EUMIC 2012, best demo award at RWW 2015, and best student paper awards at RadarConf 2020, RWW 2021 and EUMIC 2021.